Magnetophonon-resonance theory of the two-dimensional electron gas in $Al_xGa_{1-x}As/GaAs$ single heterostructures

N. Mori, H. Murata, K. Taniguchi, and C. Hamaguchi
Department of Electronic Engineering, Faculty of Engineering, Osaka University, 2-1 Yamada-Oka, Suita City, Osaka 565, Japan
(Received 12 May 1988)

The theory of the transverse magnetophonon effect in $Al_xGa_{1-x}As/GaAs$ single heterostructures is developed by using the Kubo formula and Fang-Howard trial function. The oscillatory magnetoconductivity is evaluated by harmonic analysis including Landau-level broadening. The general oscillatory structure of the magnetoresistivity is shown to depend on ω_c and ω_0, the cyclotron and optical-phonon frequencies, as $\Delta\rho \sim \sum_{r=1}^{+\infty} \exp(-2\pi r\gamma)\cos(2\pi r\omega_0/\omega_c)$ for the case of a Lorentzian-type density of states, where the damping parameter γ is determined by the Landau-level broadening and given by $\gamma = 2\Gamma/\hbar\omega_c$ with the Landau-level broadening Γ. The Landau-level broadening is evaluated for the electron scattering by optical-phonon, acoustic-phonon, remote-impurity, background-impurity, and interface-roughness scatterings. It is shown that the dominant contribution to the broadening arises from the remote-impurity scattering which results in $2\pi\gamma$ proportional to ω_0/ω_c and of the order of unity. With use of the expressions of the Landau-level broadening, the magnetophonon resonance amplitude is calculated as a function of the sheet electron density in $Al_xGa_{1-x}As/GaAs$ heterostructures, which shows a good agreement with the experimental observations by Brummell *et al.*, indicating that the damping of the magnetophonon resonance in this system is dominated by the remote-impurity scattering.

I. INTRODUCTION

In recent years electrical and optical properties of the two-dimensional electron gas (2D EG) in heterostructures and metal-oxide-semiconductor (MOS) inversion layers have received great attention.[1] Extremely high electron mobility has been achieved in modulation-doped heterostructures[2-4] and attracted applications of the heterostructures to high speed electron devices. Transport properties at both low and high electric fields have been studied from experimental and theoretical points of views. It is evident that the electron transport in heterostructures is governed by electron-phonon interaction and impurity scattering. Various kinds of measurements including Hall effect and calculations such as Monte Carlo simulation have been performed to clarify the transport properties, but still unresolved properties exist.

The magnetophonon resonance (MPR) effect is known to provide detailed information of electron-phonon interactions in semiconductors.[5-9] The MPR is caused by resonant scattering of electrons between Landau levels by absorbing or emitting longitudinal optical (LO) phonons and therefore magnetoresistance exhibits periodic oscillations in reciprocal magnetic fields. From the analysis of oscillatory magnetoresistance due to MPR we obtain effective mass or phonon energy. Earlier work of the MPR in 2D EG systems is reviewed by Nicholas *et al.*[8,9] and thus we mention only the investigations about $Al_xGa_{1-x}As/GaAs$ single heterostructures reported up to now, because we are concerned with magnetophonon effects in $Al_xGa_{1-x}As/GaAs$ single heterojunctions in this paper. Measurements of MPR have been performed first by Tsui *et al.*[10] in heterostructures of $Al_xGa_{1-x}As/GaAs$, where they obtained magnetophonon mass of $(0.077\pm0.004)m_0$. Engler *et al.*[11] carried out MPR measurements in a modulation-doped single heterostructure of $Al_xGa_{1-x}As/GaAs$ and obtained magnetophonon mass of $(0.071\pm0.0015)m_0$, which is heavier than the bulk effective mass of $0.067m_0$ and explained in terms of the conduction-band nonparabolicity. Such a heavy magnetophonon mass was also observed by Kido *et al.*[12] who obtained the mass of $0.0745m_0$. Englert *et al.* have also reported the temperature dependence of the oscillation amplitude of MPR which exhibits maximum at 210 K. Brummell *et al.*,[13] combining cyclotron and MPR experiments on $Al_xGa_{1-x}As/GaAs$ heterojunctions, found that the magnetophonon resonance results yield phonon frequencies significantly below the bulk GaAs LO phonon values, suggesting interaction of the electrons with phonons associated with the interface. Brummell *et al.*[14] have studied MPR in $Al_xGa_{1-x}As/GaAs$ heterojunctions as a function of temperature, electron concentration, and magnetic field orientation. One of the most interesting features is that the amplitude decreases rapidly with increasing carrier concentration. They explained this feature in terms of screening effect, where the screening reduces the strength of the electron-optic phonon coupling and the relative importance of transition occurring between higher Landau levels will increase. Grégoris *et al.*[15] have made measurements of MPR under hydrostatic pressure and found that the magnetophonon effective mass and oscillation amplitude increases with increasing the pressure. Leadley *et al.*[16] observed hot-electron MPR in $Al_xGa_{1-x}As/GaAs$ heterojunc-

tions between 30 and 100 K, and discussed their temperature and electric field dependence.

Theoretical studies of the MPR effect in single heterostructures have also been made by several authors. Lassnig and Zawadzki[17] reported numerical calculations of MPR conductivity in $Al_xGa_{1-x}As/GaAs$ single heterostructures, where they used the trial function of Fang-Howard[18] and gave magnetoconductivity in integral form. The present authors[19] have carried out a similar analysis by using the wave functions obtained by solving Schrödinger and Poisson equations self-consistently. These two studies are based on incorrect assumption of the density of states, resulting in Landau-level broadening twice of the correct value. Warmenbol *et al.*[20] investigated hot-electron MPR in $Al_xGa_{1-x}As/GaAs$ heterostructures using the momentum balance equation approach and found that the MPR maxima convert into minima at high electric fields.

It is well known that the formula derived by Barker[21] explains the oscillatory structures of the MPR in bulk semiconductors. Analysis of the MPR effect using this formula provided important information of the electron–LO-phonon interaction and Landau-level broadening. Recently Barker's treatment was extended to the case of MPR in crossed high electric and high magnetic fields by the present authors,[22] and the sign reversal of the MPR extrema at high electric fields was explained quantitatively. After Barker's formula came out, quantitative analyses became possible and a great progress in the MPR effects resulted. It is, therefore, desired to derive an expression of magnetoconductivity valid for 2D EG in single heterostructures. When we get such an expression, we can deal with MPR effects in the same way as in bulk (three-dimensional) semiconductors.

The purpose of this paper is to derive oscillatory magnetoconductivity of 2D EG in single heterostructures theoretically and to discuss Landau-level broadening. In Sec. II we present the derivation of an analytical expression of the magnetoconductivity, where we use Fang-Howard trial function for the wave function of 2D EG confined in the $Al_xGa_{1-x}As/GaAs$ interface and assume that the electron–LO-phonon interaction is governed by Fröhlich Hamiltonian. We find that the obtained expression shows a good agreement with the experimental results of MPR in single heterostructures. In Sec. III we calculate Landau-level broadening due to LO phonon, acoustic deformation, remote-impurity, background-impurity, and interface-roughness scatterings. We show that the remote-impurity scattering dominates the broadening effect in the structures we are interested in. In Sec. IV we calculate the Landau-level broadening as a function of carrier concentration and explain the concentration dependence of the MPR oscillation amplitude reported by Brummell *et al.*[14]

II. MAGNETOPHONON CONDUCTIVITY OF 2D EG IN SINGLE HETEROJUNCTIONS

A. Analytical expression of the transverse magnetoconductivity

In this section, an analytical expression of the transverse magnetophonon conductivity of 2D EG in single heterojunctions is developed by solving the Kubo formula[23] to include Landau-level broadening. We calculate the magnetoconductivity for three different types of the density of states of each Landau level, Lorentzian, Gaussian, and elliptic types of the density of states.

The transverse magnetoconductivity σ_{xx} is given by the Kubo formula[17,21,23]

$$\sigma_{xx}=e^2\beta\int_{-\infty}^{+\infty}dE\sum_q\frac{2\pi}{\hbar}(l^2q_y)^2N_0(1+N_0)[f(E)-f(E+\hbar\omega_0)]\times\sum_{\nu,\nu'}\delta(E+\hbar\omega_0-E_\nu)\delta(E-E_{\nu'})\,|\langle\nu'|C^*(q)e^{-iq\cdot r}|\nu\rangle|^2\,, \tag{2.1}$$

where $\beta=1/k_BT$, k_B is Boltzmann constant, T is the lattice temperature, N_0 is the Bose-Einstein distribution function of LO phonons with energy $\hbar\omega_0$ and wave vector q, $f(E)$ is the Fermi-Dirac distribution function of electrons, e is the magnitude of electronic charge, $\hbar$ is Planck constant divided by 2π, and $l=(\hbar/eB)^{1/2}$ is the cyclotron radius. The interaction potential $|C(q)|^2$ is given by the Fröhlich interaction potential

$$|C(q)|^2=4\pi\alpha\hbar(\hbar\omega_0)^{3/2}(2m^*)^{-1/2}q^{-2} \tag{2.2}$$

and α is the dimensionless coupling constant given by

$$\alpha=\frac{e^2}{4\pi\epsilon_0\hbar}\left[\frac{m^*}{2\hbar\omega_0}\right]^{1/2}\left[\frac{1}{\kappa_\infty}-\frac{1}{\kappa_0}\right], \tag{2.3}$$

where m^* is the effective mass of an electron and $\kappa_0\epsilon_0$ and $\kappa_\infty\epsilon_0$ are the static and high-frequency dielectric constant, respectively. When the electric quantization (confinement of the electrons) is taken in the z direction and the Landau magnetic quantization in the (x,y) plane, the eigenfunctions of an electron $|\nu\rangle$ and the eigenvalues E_ν are given by

$$\langle r|\nu\rangle=\langle r|N,X_\nu\rangle=\phi_N(x-X_\nu)\exp(ik_yy)\xi_0(z) \tag{2.4}$$

and

$$E_\nu=E_N=(N+\tfrac{1}{2})\hbar\omega_c+E_0^s\,, \tag{2.5}$$

where $\phi_N(x)$ are simple harmonic-oscillatorlike solutions ($N=0,1,2,\ldots$), $X_\nu=-l^2k_y$ are the center coordinates of

cyclotron motion, and E_0^s is the lowest subband energy of 2D EG. The wave function of the z direction is taken to be the Fang-Howard variational form[18]

$$\xi_0(z)=\left[\frac{b^3}{2}\right]^{1/2} z e^{-bz/2}, \tag{2.6}$$

where

$$b=\left[\frac{12m^*e^2}{\kappa_0\epsilon_0\hbar^2}(N_{\rm depl}+\tfrac{11}{32}N_s)\right]^{1/3} \tag{2.7}$$

and $N_{\rm depl}$ and N_s are the depletion charge density and the sheet electron density, respectively.

In the case of the two-dimensional system, magneto-phonon conductivity given by Eq. (2.1) diverges under resonance condition through the delta function which reflects the singularities of the density of the states.[17] In real systems, however, the singularities of the density of states are damped due to electron scattering, inhomogeneities of the system, etc. and the broadening of the electronic states removes the divergence of the magnetoconductivity. Barker[21] introduced the Lorentzian type of broadening to remove the divergence. In this paper we take into account three different types of broadening, replacing the delta functions $\delta(E)$ in Eq. (2.1) with the suitable damped representations $\delta_\Gamma(E)$ characterized by the Landau-level broadening width Γ. They are Lorentzian, Gaussian, and elliptic.

At higher temperatures such as $k_BT\gg\Gamma$, the Fermi distributions vary only slowly as a function of the energy relative to the spectral functions of the Landau levels. In that case, we obtain

$$\begin{aligned}\sigma_{xx}=\frac{e^2}{\hbar}\bar{\sigma}_0\sum_{N,N'}&[f(E_{N'})-f(E_{N'}+\hbar\omega_0)]\\&\times\langle\delta_{\bar{\Gamma}}(\bar{E}_{N'}+\bar{\omega}_0-\bar{E}_N)\rangle\\&\times\int_0^{+\infty}d\zeta\int_{-\infty}^{+\infty}d\eta\frac{\zeta}{\zeta+\eta^2}|J_{N,N'}(\zeta)|^2\\&\times|\langle\xi_0(z)|e^{-iq_zz}|\xi_0(z)\rangle|^2,\end{aligned} \tag{2.8}$$

$$\bar{\sigma}_0=\frac{1}{2\sqrt{2}}N_0(1+N_0)(\beta\hbar\omega_0)\left[\frac{e^2m^*l}{h^2\epsilon_0}\right]\left[\frac{1}{\kappa_\infty}-\frac{1}{\kappa_0}\right], \tag{2.9}$$

where

$$|J_{N,N'}(\zeta)|^2=\frac{N_n!}{N_m!}\zeta^{N_m-N_n}e^{-\zeta}|L_{N_n}^{N_m-N_n}(\zeta)|^2. \tag{2.10}$$

$N_n=\min\{N,N'\}$, $N_m=\max\{N,N'\}$, $L_p^q(\zeta)$ are the associated Laguerre polynomials and

$$\langle\delta_\Gamma(E)\rangle=\int_{-\infty}^{+\infty}\delta_\Gamma(E'-E)\delta_\Gamma(E')dE' \tag{2.11}$$

is the effective spectral density function. In Eq. (2.8) we have used dimensionless quantities defined as $\zeta=l^2(q_x^2+q_y^2)/2=l^2Q^2/2$, $\eta=lq_z\sqrt{2}$, $\bar{E}_n=E_n/\hbar\omega_c$, $\bar{\Gamma}=\Gamma/\hbar\omega_c$, and $\bar{\omega}_0=\omega_0/\omega_c$, where $\hbar\omega_c=\hbar eB/m^*$ is the cyclotron energy of an electron.

In the case of bulk materials and at extremely strong magnetic fields, the electronic wave functions have small absolute values of momentum components parallel to the applied magnetic field and the major contribution to the transverse magnetoconductivity comes from processes involving small momentum transfer along the magnetic field. Therefore we can neglect the q_z dependence in the interaction potential given by Eq. (2.2), and the term $\zeta/(\zeta+\eta^2)$ is approximated by unity as done by Barker.[21] However, in the case of single heterojunctions, electrons are confined in the region of the order $1/b$ [b is the variational parameter given by Eq. (2.7)] and "the momentum transfer along the magnetic field (z direction)" is not always small. The average of squared momentum transfer along the z direction is estimated as

$$\langle q_z^2\rangle=\int q_z^2|\langle\xi_0|e^{iq_zz}|\xi_0\rangle|^2dq_z\Big/\int|\langle\xi_0|e^{iq_zz}|\xi_0\rangle|^2\times dq_z=b^2/3 \tag{2.12}$$

and the average of squared momentum transfer in (x,y) plane is given by $\langle Q^2\rangle=2m^*\omega_0/\hbar$. Using these average values, we approximate the term $\zeta/(\zeta+\eta^2)$ appearing in Eq. (2.8) by $(1+\chi/3)^{-1}$, where χ is $(\hbar^2b^2/2m^*)/(\hbar\omega_0)$. Performing the integrations with respect to ζ and η in Eq. (2.8), we obtain

$$\sigma_{xx}=\frac{e^2}{\hbar}\bar{\sigma}_0\left[1+\frac{\chi}{3}\right]^{-1}\frac{3}{8}\pi\bar{b}\sum_{N,N'}[f(E_{N'})-f(E_{N'}+\hbar\omega_0)]\times\langle\delta_{\bar{\Gamma}}(\bar{E}_{N'}+\bar{\omega}_0-\bar{E}_N)\rangle, \tag{2.13}$$

where $\bar{b}$ is dimensionless variational parameter defined as $lb/\sqrt{2}$.

Since we introduced broadening in the delta function, the divergence at the resonance condition is removed, and instead the right-hand side of Eq. (2.13) exhibits maxima at the resonance conditions $P=N'-N$ and $\delta^P\to0$, or $P=N'-N-1$ and $\delta^P\to1$, where we defined P as the maximum integer contained in $\bar{\omega}_0$ and δ^P as the departure from resonance, that is $\delta^P=\bar{\omega}_0-P$. Retaining these terms alone and carrying out harmonic analysis, we obtain the oscillatory term of transverse magnetoresistivity $\Delta\rho$

$$\frac{\Delta\rho}{\rho_0}=\overline{\Delta\rho}\,\bar{\rho}_{\rm osc}, \tag{2.14}$$

$$\overline{\Delta\rho}=\frac{3}{2^7\pi}\left[1+\frac{\chi}{3}\right]^{-1}N_0(1+N_0)\left[\frac{\omega_0^2\tau_0m^*}{N_s\hbar}\right]\times\left[\frac{\beta e^2b}{\epsilon_0}\right]\left[\frac{1}{\kappa_\infty}-\frac{1}{\kappa_0}\right]\Theta, \tag{2.15}$$

where

$$\bar{\rho}_{\rm osc}=2\sum_{r=1}^{+\infty}\cos(2\pi r\bar{\omega}_0)\int_{-1}^{1}\langle\delta_{\bar{\Gamma}}(x)\rangle\cos(2\pi rx)dx \tag{2.16}$$

and

$$\Theta=\bar{\omega}_0^{-1}\sum_N [f(E_N)-f(E_N+\hbar\omega_0)] . \quad (2.17)$$

The term Θ is almost independent of the magnetic field and remains in the range between 0 and 1. In these equations, $\rho_0=m^*/N_s e^2\tau_0$ and τ_0 are the transverse magnetoresistivity and the relaxation time at vanishing magnetic field, respectively, and $x=E/\hbar\omega_0$. In deriving magnetoresistivity from magnetoconductivity we used the following relation, which is valid in the strong quantized regime:

$$\rho_{xx}=\left[\frac{m^*\omega_c}{N_s e^2}\right]\sigma_{xx} . \quad (2.18)$$

Next we calculate the magnetophonon resistivity from Eq. (2.14) using three types of the density of states, Lorentzian, Gaussian, and elliptic types.

1. Lorentzian density of states

When we assume the damped function $\delta_\Gamma(E)$ to be Lorentzian

$$\delta_\Gamma(E)=\delta_\Gamma^L(E)\equiv\frac{1}{\pi}\frac{\Gamma}{E^2+\Gamma^2} , \quad (2.19)$$

the effective spectral density function $\langle\delta_\Gamma^L(E)\rangle$ is reduced to Lorentzian form with the broadening width of 2Γ, and given by

$$\langle\delta_\Gamma^L(E)\rangle=\frac{1}{\pi}\frac{2\Gamma}{E^2+(2\Gamma)^2}\equiv\delta_{2\Gamma}^L(E) . \quad (2.20)$$

Using these relations and extending the upper and lower limits of integration in Eq. (2.16) to infinity,[21] we get the oscillatory part of the transverse resistivity as

$$\frac{\Delta\rho}{\rho_0}=2\overline{\Delta\rho}\sum_{r=1}^{+\infty}\exp(-2\pi r\gamma)\cos(2\pi r\bar{\omega}_0) , \quad (2.21)$$

where $\gamma=2\Gamma/\hbar\omega_c$ is the damping parameter. We have to note here that the damping parameter is twice of that defined by Barker.[21] The difference of factor 2 arises from different approximation of the spectral density.

2. Gaussian density of states

When the damped function $\delta_\Gamma(E)$ is given by Gaussian form

$$\delta_\Gamma(E)=\delta_\Gamma^G(E)\equiv\frac{1}{(2\pi\Gamma^2)^{1/2}}\exp\left[-\frac{E^2}{2\Gamma^2}\right] , \quad (2.22)$$

we get the effective spectral density function as Gaussian form with the broadening width $\sqrt{2}\Gamma$

$$\langle\delta_\Gamma^G(E)\rangle=\frac{1}{\sqrt{\pi}2\Gamma}\exp\left[-\left[\frac{E}{2\Gamma}\right]^2\right]\equiv\delta_{\sqrt{2}\Gamma}^G(E) , \quad (2.23)$$

and the oscillatory part of the transverse magnetoresistivity as

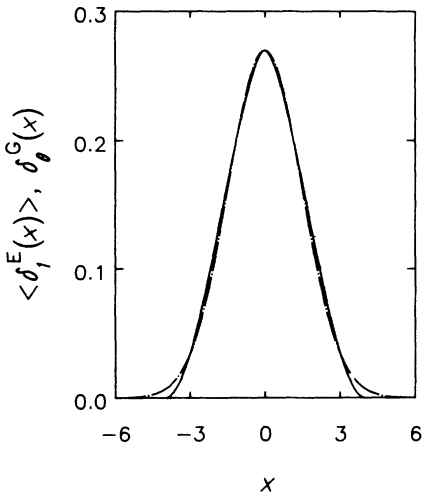

FIG. 1. The effective spectral density function of the elliptic form (solid curve) is compared with the function of Gaussian form (dash-dotted line). The width of the elliptic function is unity, and the width of the Gaussian function is $\theta=2^{1/2}3\pi^{3/2}/2^4$.

$$\frac{\Delta\rho}{\rho_0}=2\overline{\Delta\rho}\sum_{r=1}^{+\infty}\exp[-(\pi r\gamma)^2]\cos(2\pi r\bar{\omega}_0) , \quad (2.24)$$

where we extended the limits of integration in Eq. (2.16) to infinity.

3. Elliptic density of states

When we assume the damped function $\delta_\Gamma(E)$ to be elliptic

$$\delta_\Gamma(E)=\delta_\Gamma^E(E)\equiv\frac{1}{\pi\Gamma}\left[1-\left[\frac{E}{2\Gamma}\right]^2\right]^{1/2} , \quad (2.25)$$

the effective spectral density function is expressed by the following formula:

$$\langle\delta_\Gamma^E(E)\rangle=\Gamma^{-1}\langle\delta_1^E(x)\rangle \quad (x=E/\Gamma) . \quad (2.26)$$

The function $\langle\delta_1^E(x)\rangle$ is approximately reduced to Gaussian form with the broadening width $\theta=2^{1/2}3\pi^{3/2}/2^4$ (see Fig. 1), which is given by

$$\langle\delta_1^E(x)\rangle\cong\delta_\theta^G(x)\cong\delta_{\sqrt{2}}^G(x) . \quad (2.27)$$

Therefore we get the oscillatory part of the transverse magnetoresistivity as

$$\frac{\Delta\rho}{\rho_0}=2\overline{\Delta\rho}\sum_{r=1}^{+\infty}\exp[-(\pi r\gamma)^2]\cos(2\pi r\bar{\omega}_0) . \quad (2.28)$$

B. Comparison of the analytical expressions with the numerical calculations

Numerical calculations of magnetoresistance using the Kubo formula have been carried out by Lassnig and Zawadzki[17] and Mori and Hamaguchi.[19] Lassnig and Zawadzki evaluated magnetoresistance by using Fang-

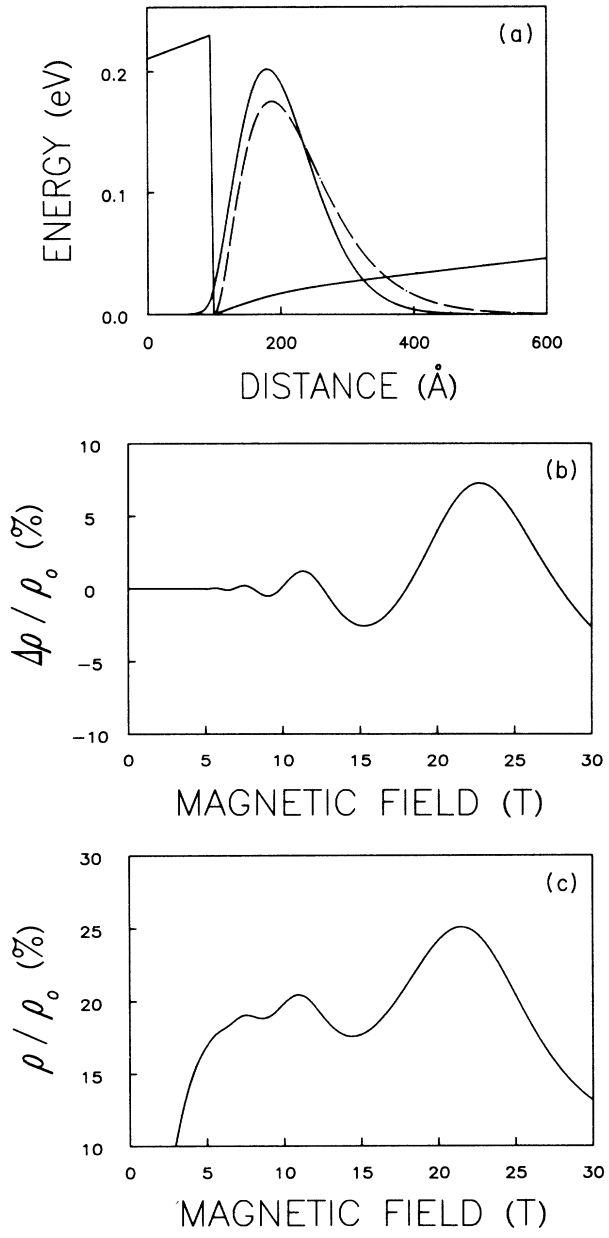

FIG. 2. (a) Comparison of the squared Fang-Howard trial function (dash-dotted curve) with the squared wave function of the lowest subband calculated by self-consistent method (solid curve), for $N_s=1\times10^{11}$ cm^{-2}, $T=220$ K, and $N_A=1\times10^{14}$ cm^{-3} which gives $N_{\rm depl}=4.5\times10^{10}$ cm^{-2}. The wave function calculated by the self-consistent method is shown along with the potential (conduction-band edge). (b) Plot of the oscillatory part of the transverse magnetophonon resisitivity normalized by the resistivity at vanishing magnetic field $\Delta\rho/\rho_0$ calculated by Eq. (2.21) for $N_s=1\times10^{11}$ cm^{-2}, $T=220$ K, and $N_{\rm depl}=4.5\times10^{10}$ cm^{-2}. The Landau-level width Γ is assumed to be 5 meV and independent of the magnetic field and the relaxation time at vanishing magnetic field is assumed to be given by $\hbar/\tau_0=1.87$ meV. (c) Plot of the transverse magnetophonon resistivity normalized by the resistivity at vanishing magnetic field ρ/ρ_0, which is numerically calculated using the results of self-consistent calculation and the method reported in Ref. 19, for $N_s=1\times10^{11}$ cm^{-2}, $T=220$ K, $N_A=1\times10^{14}$ cm^{-3}, $\Gamma=5$ meV, and $\hbar/\tau_0=1.87$ meV.

Howard trial function, where the evaluation of the Kubo formula is different from the present treatment mentioned above. Mori and Hamaguchi evaluated magnetoresistance by using eigen functions and eigen values which were obtained by solving Schrödinger and Poisson equations self-consistently. If the damping parameter is properly taken into account, the latter treatment is more accurate. It is very interesting to compare the analytical expressions obtained above with the numerical calculations. We show that the present expressions are in reasonable agreement with the numerical calculations.

First we compare the wave function obtained by the self-consistent calculation (solid curve) with the Fang-Howard trial function (dash-dotted curve) in Fig. 2(a) for $N_s=1\times10^{11}$ cm^{-2} and in Fig. 3(a) for $N_s=5\times10^{11}$

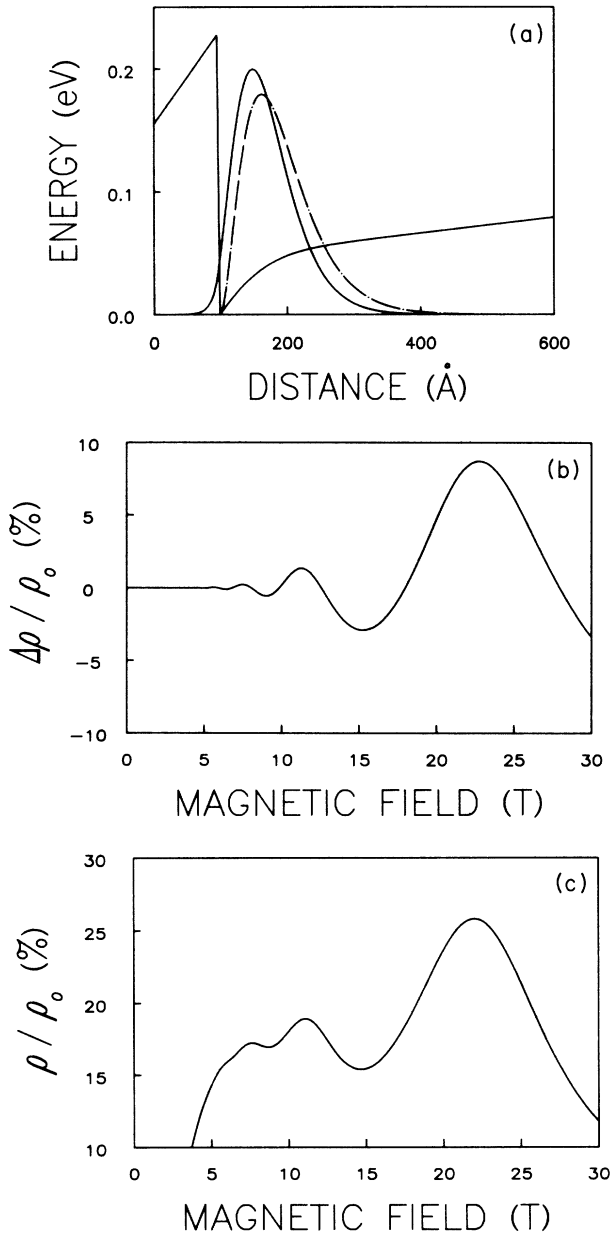

FIG. 3. Same as Fig. 2, but for $N_s=5\times10^{11}$ cm^{-2} and $N_{\rm depl}=4.6\times10^{10}$ cm^{-2} ($N_A=1\times10^{14}$ cm^{-3}).

cm^{-2}, where the wave functions of the lowest subband are shown and the lattice temperature T is 220 K. We find in Fig. 2(a) and Fig. 3(a) that both wave functions, self-consistent solutions, and Fang-Howard functions, are in good agreement with each other. Oscillatory parts of transverse magnetoresistivities calculated from Eq. (2.21) (for Lorentzian form) are shown as a function of magnetic field in Fig. 2(b) for $N_s=1\times10^{11}$ cm^{-2} and in Fig. 3(b) for $N_s=5\times10^{11}$ cm^{-2} at $T=220$ K. We assume in Fig. 2(b) and Fig. 3(b) that the Landau level is Lorentzian form with broadening 5 meV which is independent of magnetic field. Numerical calculations of the magnetoresistivity using the self-consistent wave functions were carried out in the same manner reported elsewhere,[19] where the density of states is assumed to be of Lorentzian form with constant broadening (5 meV) and only the wave functions of the lowest subband shown in Fig. 2(a) and Fig. 3(a) are used. The obtained results are shown in Fig. 2(c) for $N_s=1\times10^{11}$ cm^{-2} and in Fig. 3(c) for $N_s=5\times10^{11}$ cm^{-2} at $T=220$ K. We find in these figures that the oscillatory structures of the magnetoresistance are in good agreement. It should be noted here that the numerical curves contain nonoscillatory background component of the magnetoresistivity.

III. LANDAU-LEVEL BROADENING

In this section we examine the Landau-level broadening due to remote-impurity, background-impurity, LO phonon, acoustic deformation, and interface-roughness scatterings. The presence of two or more scattering processes of similar strength considerably complicates the evaluation of the irreducible self-energy and is not considered here. We consider screening effect only for the remote-impurity, background-impurity, and interface-roughness scatterings.

A. Evaluation of the Landau level broadening

1. Remote-impurity scattering

When the spatial distribution of impurities are given by $N_i(z_i)$, where $N_i(z_i)$ is the concentration of ionized impurities per unit volume, the self-energy of the Green's function $G_N(E)=[E-E_N-\Sigma_N(E)]^{-1}$ is given by[24]

$$\Sigma_N(E)=\sum_{N'}\int\frac{d^2Q}{(2\pi)^2}N_i(Q)\,|\,v(Q)\,|^2\,|\,J_{N,N'}(\zeta)\,|^2G_{N'}(E)\ , \tag{3.1}$$

where

$$N_i(Q)=\int dz_i\,N_i(z_i)\,|\,F_Q(z_i)\,|^2\ , \tag{3.2}$$

$$|\,F_Q(z_i)\,|=\int|\,\xi_0(z)\,|^2e^{-Q|z-z_i|}\,dz\ , \tag{3.3}$$

$$|\,v(Q)\,|=\frac{e^2}{2\kappa_0\epsilon_0\epsilon(Q)Q}\ , \tag{3.4}$$

and $\epsilon(Q)$ is the static dielectric function which is assumed to be given by Thomas-Fermi model,[1,25] that is

$$\epsilon(Q)=1+F(Q)\frac{Q_s}{Q}\ , \tag{3.5}$$

and

$$Q_s=\frac{e^2}{2\kappa_0\epsilon_0}\int D(E)\left[-\frac{\partial f(E)}{\partial E}\right]dE\ , \tag{3.6}$$

$$F(Q)=\int\int|\,\xi_0(z_1)\,|^2\,|\,\xi_0(z_2)\,|^2e^{-Q|z_1-z_2|}\,dz_1dz_2\ , \tag{3.7}$$

where $D(E)$ is the density of states given by

$$D(E)=\left[-\frac{1}{\pi}\right]\frac{1}{\pi l^2}\sum_N\mathrm{Im}G_N(E+i0)\ . \tag{3.8}$$

At lower temperatures such as $k_BT\ll\Gamma$, the Fermi distributions vary rapidly as a function of the energy relative to the spectral functions of the Landau levels. Therefore the dielectric response of 2D EG under a strong magnetic field must be obtained within a self-consistent procedure in which the Landau-level broadening due to collisional damping from the impurities both determines and is determined by the static dielectric function of the system.[26–28] However, at higher temperatures ($k_BT\gg\Gamma$) which is the range of interest for the MPR effect, the screening parameter is determined by the thermal energy k_BT and is not affected by the minute structure of the density of states, therefore we can evaluate the Landau-level broadening due to impurity scattering and the static dielectric function, independently. In that case, under magnetic field, the screening parameter of the Thomas-Fermi model is also given by the zero magnetic form, which is written as

$$Q_s=\frac{e^2}{2\kappa_0\epsilon_0}\frac{m^*}{\pi\hbar^2}\left[1-\exp\left[-\frac{T_F}{T}\right]\right]\ , \tag{3.9}$$

where $T_F=(\pi\hbar^2/m^*k_B)N_s$ is the Fermi temperature.

Neglecting the self-energy shift, we obtain the Landau-level broadening $\Gamma_{N+P}(E_N+\hbar\omega_0)$ which determines the magnetophonon amplitudes[21]

$$\Gamma_{N+P}(E_N+\hbar\omega_0)=\sum_{N'}S_{N+P,N'}\pi\delta^L_{\Gamma_{N'}}(E_N+\hbar\omega_0-E_{N'})\ , \tag{3.10}$$

and

$$S_{N,M}=\int\frac{d^2Q}{(2\pi)^2}N_i(Q)\,|\,v(Q)\,|^2\,|\,J_{N,M}(\zeta)\,|^2\ . \tag{3.11}$$

Retaining the dominant term of Eq. (3.10) which involves $N'=N+P$ and considering the magnetophonon resonance condition ($\delta^P\to0$), we get the Landau-level broadening due to the impurity scattering and the density of states of Lorentzian form as

$$\Gamma_N^2=\int\frac{d^2Q}{(2\pi)^2}N_i(Q)\,|\,v(Q)\,|^2\,|\,J_{N,N}(\zeta)\,|^2\ , \tag{3.12}$$

and

$$D(E)=\frac{1}{\pi l^2}\sum_N \frac{1}{\pi}\frac{\Gamma_N}{(E-E_N)^2+\Gamma_N^2} . \tag{3.13}$$

Here we calculate the Landau-level broadening due to the remote-impurity scattering using Eq. (3.12), and in the next subsection we calculate the Landau-level broadening due to the background-impurity scattering using Eq. (3.12).

The spatial distribution $N_i(z_i)$ of the ionized remote impurity is assumed to be given by

$$N_i(z_i)=\begin{cases} N_i, & -(L_i+L_s)<z_i<-L_s \\ 0 \text{ otherwise} , \end{cases} \tag{3.14}$$

where L_s is the spacer layer thickness, L_i is the ionized layer thickness, and we define that the heterointerface is located at $z=0$; the GaAs layer is the positive region of z axis ($z>0$) and the $Al_xGa_{1-x}As$ layer is the negative region of z axis ($z<0$). We obtain the Nth-Landau-level broadening due to remote-impurity scattering $\Gamma_{\mathrm{RIS},N}$ as

$$\Gamma_{\mathrm{RIS},N}=\left[\frac{1}{4\pi}\left[\frac{e^2}{2\kappa_0\epsilon_0}\right]^2 N_{is}\int_0^{+\infty} d\xi \frac{1}{\epsilon^2(Q)}\frac{e^{-2\bar{L}_s\sqrt{\xi}}}{(1+\sqrt{\xi}/\bar{b})^6}\times |J_{N,N}(\xi)|^2\right]^{1/2} , \tag{3.15}$$

where $N_{is}=N_iL_i$ and $\bar{L}_s=\sqrt{2}L_s/l$. In Eq. (3.15) we use the fact that the major contribution to the Landau-level broadening comes from small momentum transfer in the (x,y) plane, small Q value, and that the term $1-\exp(-2L_iQ)$ is approximated by $2L_iQ$.

2. Background-impurity scattering

The spatial distribution of the ionized background-impurity is assumed to be

$$N_A(z_A)=\begin{cases} N_A, & 0<z_A<L_A \\ 0 \text{ otherwise} , \end{cases} \tag{3.16}$$

and we define $\bar{N}_A(Q)$ as

$$\bar{N}_A(Q)=\frac{1}{L_AN_A}\int N_A(z_A)|F_Q(z_A)|^2 dz_A = \frac{1}{L_A}\int_0^{L_A} dz_A |F_Q(z_A)|^2 . \tag{3.17}$$

In general, the Landau-level broadening width due to background-impurity scattering is smaller by an order of magnitude than the Landau-level broadening width due to remote-impurity scattering. Therefore we may evaluate $\bar{N}_A(Q)$ by interpolating between small Q and large Q limits, and we get the relation

$$\bar{N}_A(Q)=[1+\bar{\beta}I_0(\chi_A)+\bar{\beta}^2I_\infty^{-1}(\chi_A)]^{-1} , \tag{3.18}$$

and

$$I_0(\chi_A)=2\int_0^{L_A}\frac{dz_A}{L_A}\left[b\int_0^{+\infty}|\xi_0(z)|^2|z-z_A|dz\right] , \tag{3.19}$$

$$I_\infty(\chi_A)=\frac{4}{b^2}\int_0^{L_A}\frac{dz_A}{L_A}|\xi_0(z)|^4 , \tag{3.20}$$

where $\bar{\beta}=Q/b$ and $\chi_A=bL_A$.

From Eq. (3.12) and Eq. (3.18) we obtain the Nth Landau-level broadening due to background-impurity scattering $\Gamma_{\mathrm{BIS},N}$ as

$$\Gamma_{\mathrm{BIS},N}=\left[\frac{1}{4\pi}\left[\frac{e^2}{2\kappa_0\epsilon_0}\right]^2 N_AL_A\int_0^{+\infty} d\xi \frac{1}{\epsilon^2(Q)}\frac{|J_{N,N}(\xi)|^2}{1+\bar{\beta}I_0(\chi_A)+\bar{\beta}^2I_\infty^{-1}(\chi_A)}\right]^{1/2} . \tag{3.21}$$

3. LO phonon scattering

We consider a damping mechanism of the electron–LO-phonon interaction itself. A full treatment of LO phonon scattering must include the polaron mass shift, but for our purpose it suffices to absorb this correction into the cyclotron frequency and consider only the polaron decay rate.

In the case of single heterojunction, the self-energy of $G_N(E)$ is given by

$$\Sigma_N(E)=\sum_{N'} C_{N,N'}^2[N_0G_{N'}(E+\hbar\omega_0) + (1+N_0)G_{N'}(E-\hbar\omega_0)] , \tag{3.22}$$

and

$$C_{N,M}^2=\sum_q |J_{N,M}(\zeta)|^2 |\langle\xi_0|e^{iq_zz}|\xi_0\rangle|^2 |C(q)|^2 , \tag{3.23}$$

where we assumed that the electron–LO-phonon interaction is not altered by the interface. Neglecting the self-energy shift, and calculating imaginary part of the self-energy, we obtain the expression of the $\Gamma_{N+P}(E_N+\hbar\omega_0)$ as

$$\Gamma_{N+P}(E_N+\hbar\omega_0)=\sum_{N'}C_{N+P,N'}^2 \times[N_0\pi\delta_{\Gamma_{N'}}^L(E_N+2\hbar\omega_0-E_{N'}) + (1+N_0)\pi\delta_{\Gamma_{N'}}^L(E_N-E_{N'})] . \tag{3.24}$$

The terms responsible in Eq. (3.24) involve the LO phonon emission part and the absorption part. Retaining these terms alone and setting $(\zeta+\eta^2)^{-1}$ equal to $(1+\chi/3)^{-1}/\zeta$, using the argument of Sec. II, we evaluate $\Gamma_{N+P}(E_N+\hbar\omega_0)$ as

$$\Gamma_{N+P}=C^2_{N+P,N+2P}N_0\Gamma^{-1}_{N+2P}+C^2_{N+P,N}(1+N_0)\Gamma^{-1}_{N} . \tag{3.25}$$

The term $C_{N,M}$ in Eq. (3.25) depends only on the difference between N and M, explicitly

$$C^2_{N,M}=\frac{1}{|N-M|}\frac{\pi}{(2\pi)^3}\frac{3}{8}\pi b\left[1+\frac{\chi}{3}\right]^{-1} \times 4\pi\alpha\hbar(\hbar\omega_0)^{3/2}(2m^*)^{-1/2} \quad (N\neq M) . \tag{3.26}$$

Therefore we get the Landau-level broadening due to LO phonon scattering $\Gamma_{\rm OPS}$ with density of states of Lorentzian form as

$$\Gamma_{\rm OPS}=\left[\frac{3}{2^7\pi}\left[1+\frac{\chi}{3}\right]^{-1} \times\frac{e\hbar\omega_c}{\epsilon_0}\left[\frac{1}{\kappa_\infty}-\frac{1}{\kappa_0}\right]b(1+2N_0)\right]^{1/2} . \tag{3.27}$$

From this equation we can see that the level broadening due to LO phonon scattering is proportional to $\alpha^{1/2}$, where α is the dimensionless coupling constant given by Eq. (2.3).

4. *Acoustic-phonon scattering*

The self-energy of $G_N(E)$ is given by

$$\Sigma_N(E)=\frac{D^2k_BT}{2ds_l^2}\sum_q\sum_{N'}|J_{N,N'}(\zeta)|^2\,|\langle\xi_0|e^{iqz^z}|\xi_0\rangle|^2 \times[G_{N'}(E+\hbar s_l q)+G_{N'}(E-\hbar s_l q)] , \tag{3.28}$$

where D is the deformation potential, s_l is the velocity of sound, and d is the crystal density. In Eq. (3.28) we have used the approximation $N_q+\frac{1}{2}\pm\frac{1}{2}\cong k_BT/\hbar\omega_q=k_BT/\hbar s_l q$, where N_q is the Bose-Einstein distribution for acoustic phonons with energy $\hbar\omega_q$ and wave vector q. Using the elastic scattering approximation, and using the argument of Sec. III A 1, we get the Landau-level broadening due to acoustic-phonon scattering $\Gamma_{\rm APS}$ as

$$\Gamma_{\rm APS}=\left[\frac{3}{2^5\pi}\frac{m^*bD^2}{\hbar ds_l^2}k_BT\hbar\omega_c\right]^{1/2} \tag{3.29}$$

with the density of states as Lorentzian form.

5. *Interface-roughness scattering*

When we consider the interface-roughness scattering, the self-energy of $G_N(E)$ is given by

$$\Sigma_N(E)=\sum_{N'}\int\frac{d^2Q}{(2\pi)^2}\pi\left[\frac{\Delta\Lambda e^2}{2\kappa_0\epsilon_0\epsilon(Q)}N_{\rm eff}\right]^2\exp(-\tfrac{1}{4}Q^2\Lambda^2) \times|J_{N,N'}(\zeta)|^2G_{N'}(E) , \tag{3.30}$$

where Δ is the mean-square deviation of the height of the roughness and Λ is the lateral spatial decay rate of the roughness.[29] Using the argument of Sec. III A 1, we obtain the Nth-Landau-level broadening due to interface-roughness scattering $\Gamma_{{\rm IRS},N}$ with the density of states of Lorentzian form as

$$\Gamma_{{\rm IRS},N}=\Delta\Lambda N_{\rm eff}\frac{e^2}{2\kappa_0\epsilon_0\epsilon(Q)l} \times\left\{\tfrac{1}{2}\int_0^{+\infty}d\zeta\frac{\zeta}{\epsilon^2(Q)}\exp\left[-\frac{1}{2}\left[\frac{\Lambda}{l}\right]^2\zeta\right] \times|J_{N,N}(\zeta)|^2\right\}^{1/2} . \tag{3.31}$$

B. Temperature, magnetic field, and sheet electron concentration dependence of the Landau-level broadening

In this section, we calculate the Landau-level broadening due to the electron scatterings mentioned above as a function of the temperature, magnetic field, and sheet electron concentration. In heterojunctions the electrons confined in the interface region are supplied from the

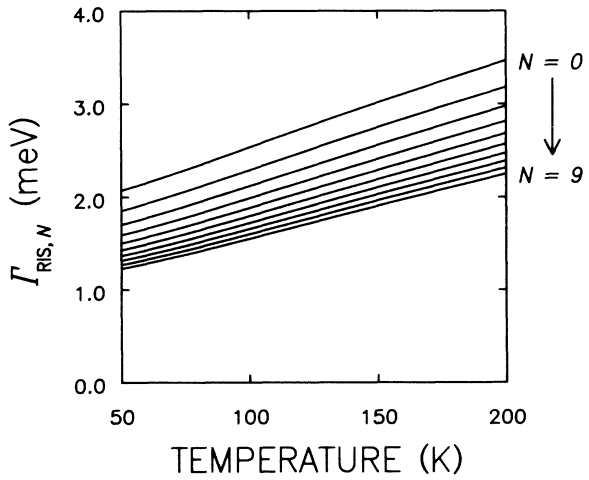

FIG. 4. Temperature dependence of the Nth-Landau-level broadening due to remote-impurity scattering $\Gamma_{{\rm RIS},N}$, with the Landau quantum number $N=0\sim9$ as a parameter for $N_s=3\times10^{11}$ cm^{-2}, $N_{\rm depl}=5\times10^{10}$ cm^{-2}, $L_s=100$ Å, and $B=7.38$ T (corresponds to the MPR peak for $P=3$). The broadening $\Gamma_{{\rm RIS},N}$ is larger for larger values of N and the temperature dependence of $\Gamma_{{\rm RIS},N}$ is almost independent of N.

TABLE I. The parameters used for the calculations.

Effective mass	m^*/m_0	
for self-consistent calculation		0.067
for cyclotron energy		0.07
LO phonon energy	$\hbar\omega_0$	36.6 meV
Static dielectric constant	κ_0	12.9
High-frequency dielectric constant	κ_∞	10.9
Density of GaAs	d	5.37 g/cm^3
Speed of sound	s_l	5.24×10^5 cm/s
Deformation potential	D	7 eV
The mean-square deviation of the height of the roughness	Δ	5 Å
The lateral spatial decay rate of the roughness	Λ	15 Å

donors in the $Al_{1-x}Ga_xAs$ layer. Taking into account the background impurities in GaAs (assumed to be acceptors) the impurity densities are determined by the charge neutrality condition, which is given by

$$N_{is}=N_A L_A+N_s$$
$$=N_{\text{depl}}+N_s\ , \tag{3.32}$$

where $N_{is}=N_iL_i$, N_i is the impurity (donor) density intentionally doped in $Al_xGa_{1-x}As$ layer, L_i is the thickness of the ionized layer, N_A is the background impurity (acceptor) density, L_A is the depletion length in GaAs, and N_s is the sheet electron density at the interface.

First, we consider the Landau quantum number N dependence of the Landau-level broadening due to the remote-impurity scattering, $\Gamma_{\text{RIS},N}$. In Fig. 4 we show the temperature dependence of $\Gamma_{\text{RIS},N}$ as the parameter of the Landau quantum number $N=0\sim9$ for depletion charge density $N_{\text{depl}}=5\times10^{10}$ cm^{-2}, sheet electron density $N_s=3\times10^{11}$ cm^{-2}, spacer layer thickness $L_s=100$ Å, and magnetic field $B=7.38$ T (which corresponds to the third resonance condition, that is $P=3$), other parameters used in the calculation is summarized in Table I. We find in Fig. 4 that $\Gamma_{\text{RIS},N}$ decrease monotonously with increasing N, and that the temperature dependence of $\Gamma_{\text{RIS},N}$ is almost independent of N. We may show that the magnetic field and sheet electron density dependence of $\Gamma_{\text{RIS},N}$ are almost independent of N. Therefore we define Γ_{RIS} as given by $\Gamma_{\text{RIS},0}$ and in the following we consider only Γ_{RIS}. From the same argument, we define Γ_{BIS} and Γ_{IRS} as given by $\Gamma_{\text{BIS},0}$ and $\Gamma_{\text{IRS},0}$, respectively.

Secondly, we calculate the temperature dependence of the level broadening Γ_{RIS}, Γ_{BIS}, Γ_{OPS}, Γ_{APS}, and Γ_{IRS}. We show the temperature dependence of Γ_{RIS}, Γ_{OPS}, Γ_{APS}, and Γ_{IRS} in Fig. 5(a) and the temperature dependence of Γ_{BIS} in Fig. 5(b) together with Γ_{IRS} for comparison, for $B=7.38$ T, $N_{\text{depl}}=5\times10^{10}$ cm^{-2}, $N_s=3\times10^{11}$ cm^{-2}, and $L_s=100$ Å. In Fig. 5 we can see that Γ_{RIS} and Γ_{OPS} are larger than Γ_{APS}, Γ_{IRS}, and Γ_{BIS}. Since the screening effect becomes weak with increasing the tem-

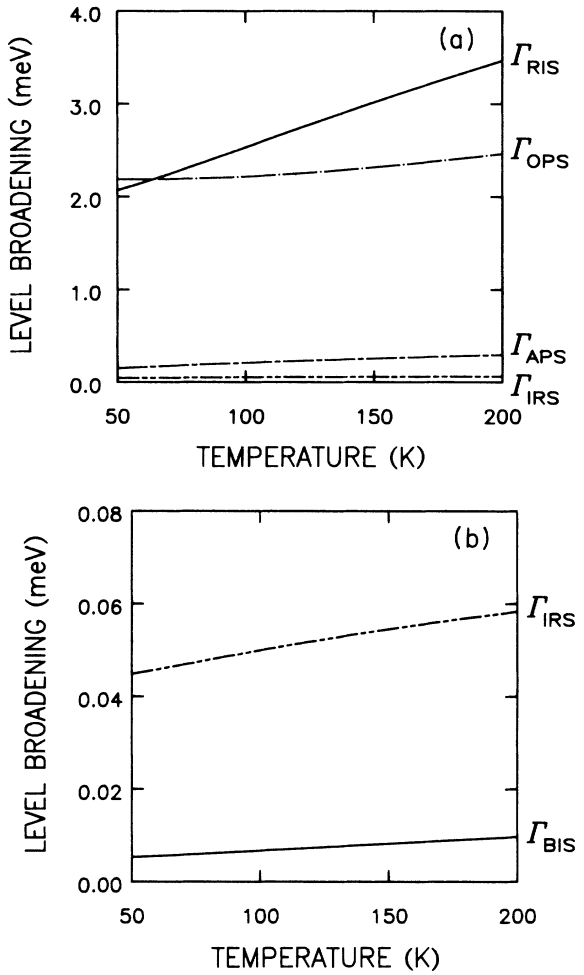

FIG. 5. (a) Temperature dependence of the Landau-level broadening due to remote-impurity scattering Γ_{RIS}, optical-phonon scattering Γ_{OPS}, acoustic-phonon scattering Γ_{APS}, and interface-roughness scattering Γ_{IRS}, and (b) temperature dependence of the Landau-level broadening due to background-impurity scattering Γ_{BIS} together with Γ_{IRS} for comparison, for $N_s=3\times10^{11}$ cm^{-2}, $N_{\text{depl}}=5\times10^{10}$ cm^{-2}, $L_s=100$ Å and $B=7.38$ T (corresponds to the MPR peak for $P=3$).

perature, we find in Fig. 5 that the level broadening due to impurity scattering and due to interface-roughness scattering become large with increasing the temperature. The level broadening due to LO phonon scattering Γ_{OPS} depends on the temperature as $(1+2N_0)^{1/2}$ ($N_0<1$ for LO phonon energy 36.6 meV and the temperature range of interest for the MPR effect), and therefore the temperature dependence of Γ_{OPS} is weaker than that of Γ_{RIS}. The level broadening due to acoustic deformation scattering depends on temperature as $T^{1/2}$, which reflects the distribution of acoustic phonon N_q is mach larger than unity and N_q are in proportion to the temperature.

Thirdly, we calculate the magnetic field dependence of the level broadening Γ_{RIS}, Γ_{BIS}, Γ_{OPS}, Γ_{APS}, and Γ_{IRS}. We show the magentic field dependence of Γ_{RIS}, Γ_{OPS}, Γ_{APS}, and Γ_{IRS} in Fig. 6(a) and the magnetic field dependence of Γ_{BIS} together with Γ_{IRS} for comparison, for $T=180$ K, $N_{depl}=5\times10^{10}$ cm^{-2}, $N_s=3\times10^{11}$ cm^{-2}, and $L_s=100$ Å. The level broadening Γ_{RIS} due to the remote-impurity scattering shows weaker dependence of the magnetic field than Γ_{OPS} due to the LO phonon scattering where the latter is proportional to $B^{1/2}$.

Finally, we calculate the sheet electron density dependence of the level broadening Γ_{RIS}, Γ_{BIS}, Γ_{OPS}, Γ_{APS}, and Γ_{IRS}. The sheet electron density can be changed by changing the donor density in $Al_xGa_{1-x}As$ layer with a fixed spacer layer thickness, or by changing the spacer layer thickness with a fixed donor density in $Al_xGa_{1-x}As$ layer. We consider here the former case only, and in the next section we consider the latter case. The calculated sheet electron density dependence of Γ_{RIS}, Γ_{OPS}, Γ_{APS}, and Γ_{IRS} are shown in Fig. 7(a) and the calculated sheet electron density dependence of Γ_{BIS} are shown in Fig. 7(b) together with Γ_{IRS} for comparison, for $T=180$ K,

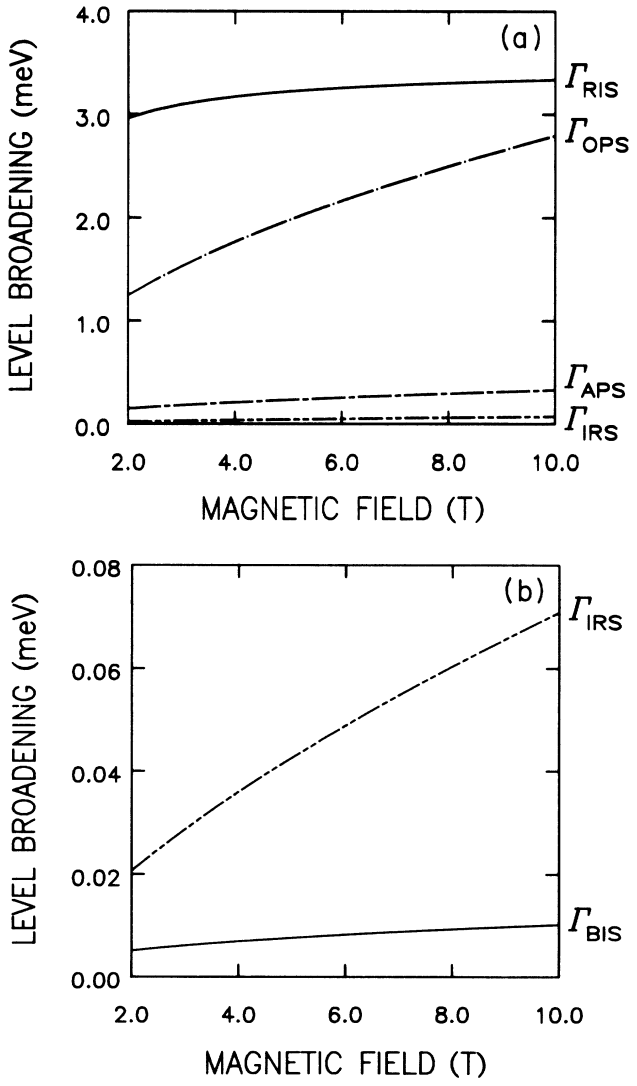

FIG. 6. (a) Magnetic field dependence of the Landau-level broadening Γ_{RIS}, Γ_{OPS}, Γ_{APS}, and Γ_{IRS}, and (b) Γ_{BIS} (Γ_{IRS} is also shown for comparison), for $N_s=3\times10^{11}$ cm^{-2}, $N_{depl}=5\times10^{10}$ cm^{-2}, $L_s=100$ Å and $T=180$ K.

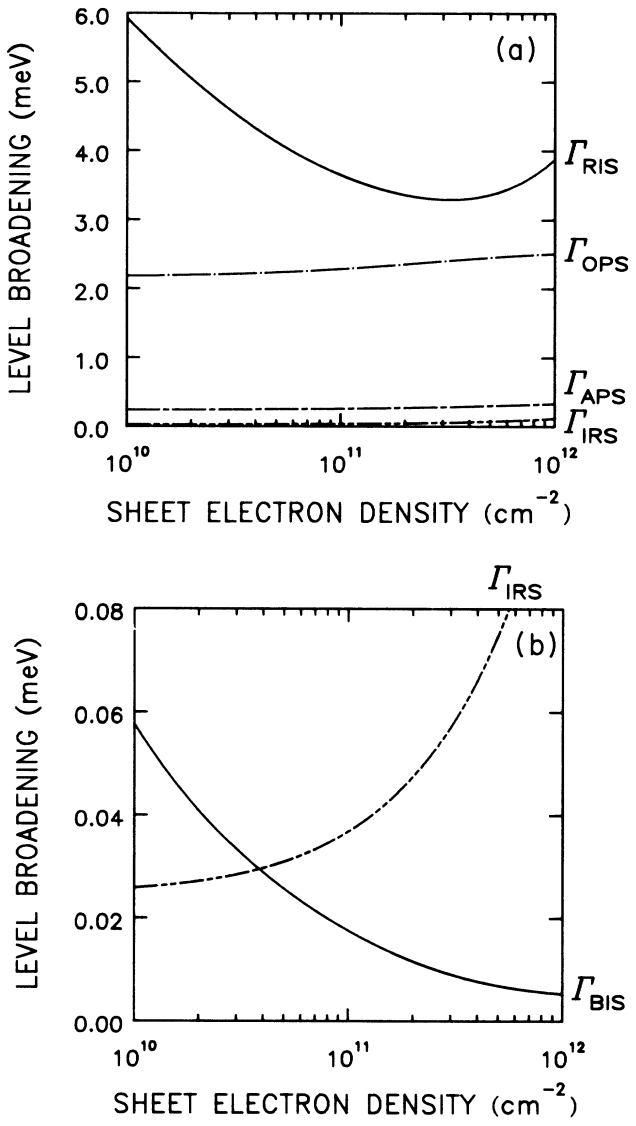

FIG. 7. (a) Sheet electron density dependence of the Landau-level broadening Γ_{RIS}, Γ_{OPS}, Γ_{APS}, and Γ_{IRS}, and (b) sheet electron density dependence of the Landau-level broadening Γ_{BIS} (Γ_{IRS} is also shown for comparison), for $N_{depl}=5\times10^{10}$ cm^{-2}, $L_s=100$ Å, $B=7.38$ T ($P=3$), and $T=180$ K.

$B=7.38$ T, $N_{depl}=5\times10^{10}$ cm^{-2}, and a fixed spacer layer thickness $L_s=100$ Å. We find in Fig. 7(a) that the level broadening due to remote-impurity scattering, Γ_{RIS}, has a minimum at around $N_s=3\times10^{11}$ cm^{-2}. The remote-impurity scattering is governed by two effects; an increase in N_{is} results in an increase in broadening, whereas an increase in N_s results in a decrease in broadening due to the screening effect. The reason why Γ_{RIS} has a minimum is explained in terms of competition of the two effects. In the region of the sheet electron density N_s less than the depletion charge density N_{depl}, the screening effect dominates and thus the increase in N_s results in a decrease of Γ_{RIS}. On the other hand in the region of sufficiently higher N_s, such as $N_s \gg N_{depl}$, the term of N_{is} dominates and thus the increase in the sheet electron density N_s is proportional to the increase in the sheet donor density N_{is}, resulting in an increase of Γ_{RIS}. It is evident from these considerations that the value of N_s which gives a minimum of Γ_{RIS} depends on the value of N_{depl}. We find in Fig. 7(a) that the broadening due to LO phonon scattering Γ_{OPS} increases with increasing the sheet electron density N_s. This feature may be explained in terms that the spatial extent of the wave function perpendicular to the heterointerface decreases and the variational parameter b increases with increasing N_s, where we neglected the screening effect for LO phonon scattering. When the screening effect of the LO phonon scattering is taken into account, the broadening Γ_{OPS} decreases slightly with increasing N_s.

IV. SHEET ELECTRON DENSITY DEPENDENCE OF THE MAGNETOPHONON AMPLITUDE

Recently Brummell *et al.*[14] have reported very interesting results of the MPR effects in $Al_xGa_{1-x}As$/GaAs heterostructures. They studied the amplitude of the MPR oscillations as a function of the sheet electron density in the range $N_s=3\times10^{10}$ cm^{-2} to 5×10^{11} cm^{-2}, using a number of different samples, and found that the amplitude decreases rapidly with increasing the sheet electron density. They attributed the decrease to the screening effect as follows. At 180 K the system is close to degenerate statistics at approximately 3×10^{11} cm^{-2} and the condition $k_BT\cong\hbar\omega_c\cong E_F$ $(B=0)$ is fulfilled. Under this condition screening effect plays a more important role, leading to a reduction in the strength of the electron-optical phonon coupling, and the magnetophonon amplitude decreases. We have to note here that the amplitude of the MPR oscillations is determined by the following two factors, the electron-optical phonon coupling constant in the preexponent $\Delta\rho$ [Eq. (2.15) and Eq. (2.21)] and the damping parameter γ (or the Landau-level broadening Γ) in the exponent [Eq. (2.21)]. Their explanation is based on the decrease in $\Delta\rho$ due to the screening effect. However, such a rapid decrease with respect to the sheet electron density cannot be explained in terms of the electron density dependence of the electron-phonon coupling constant contained in the preexponent. Instead it may be expected that the damping parameter of the Landau-level broadening in the exponent depends on the electron density or the remote-impurities, leading to exponential decrease in the amplitude with respect to the electron density. As shown in the preceding section, the Landau-level broadening is dominated by remote-impurity scattering and its electron density dependence exhibits a complicated behavior due to competition of the screening effect and number of scattering centers and/or the distribution of the remote impurities [L_s in Eq. (3.15)].

We estimate the magnetophonon amplitude using the results of Sec. II and Sec. III. The sheet electron density of the samples used by Brummell *et al.*[14] is changed by changing the spacer layer thickness and by keeping doping density constant (1.3×10^{18} cm^{-3}). The specification of their samples is reported by Foxon *et al.*[30] and the sheet electron density versus the spacer layer thickness is retraced in Fig. 8 along with the sample structure. We have to note that the sheet electron density is determined by the thickness of the spacer layers. As stated above the Landau-level broadening due to remote-impurity scattering is determined by three factors, screening effect, sheet impurity density N_{is}, and spacer layer thickness L_s. An increase in N_{is} and a decrease in L_s result in an increase in the broadening Γ_{RIS}. This is the case observed by Brummell *et al.*[14] Using the result of Fig. 8 we calculated the Landau-level broadening due to the remote-impurity scattering Γ_{RIS}, which is shown in Fig. 9. We

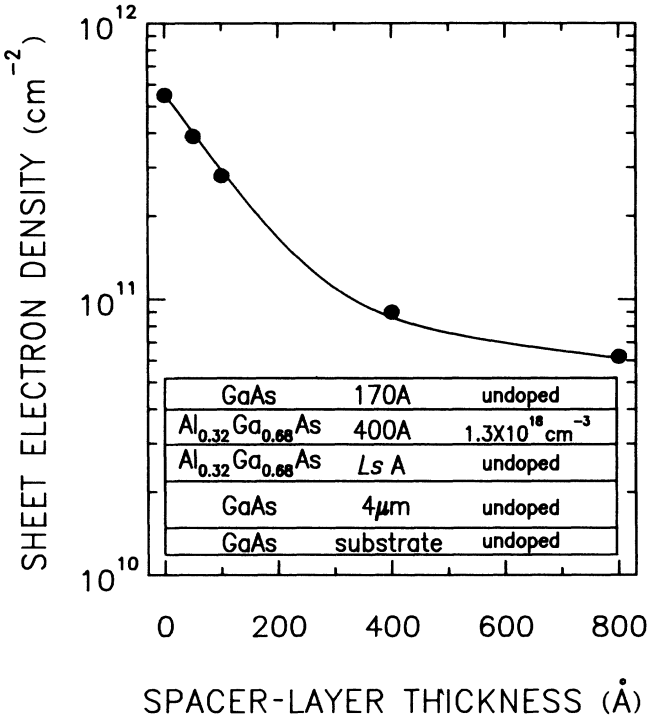

FIG. 8. The sheet electron density as a function of the spacer layer thickness, which is reproduced using the result reported by Foxon *et al.* (Ref. 30) at temperature 77 K. The samples are used for the MPR experiments by Brummell *et al.* (Ref. 14). The $Al_xGa_{1-x}As$/GaAs heterostructures used by them are shown in the inset.

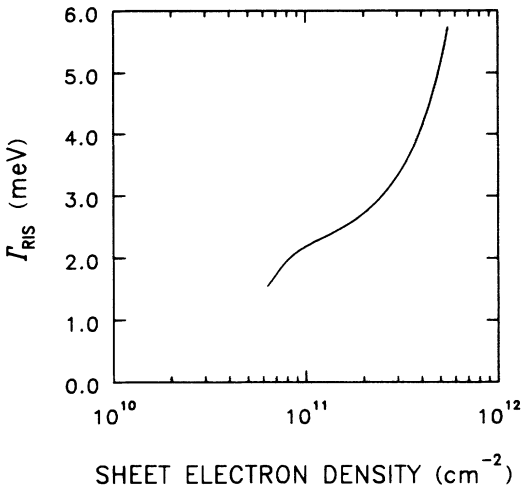

FIG. 9. The Landau-level broadening due to remote-impurity scattering Γ_{RIS} as a function of sheet electron density, where the broadening is estimated by taking account of the relation between the spacer layer thickness and the sheet electron density reported by Foxon *et al.* (Ref. 30) (Fig. 8).

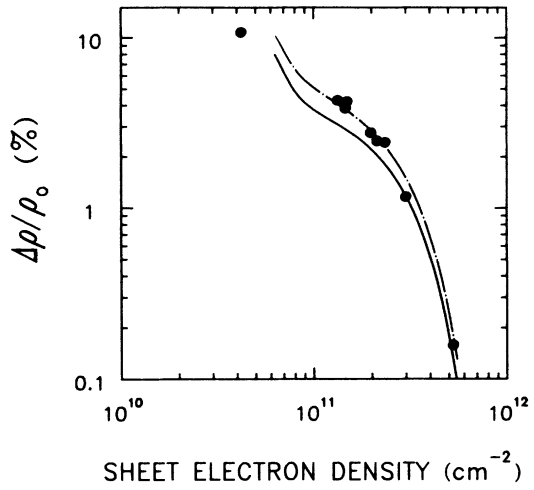

FIG. 10. The sheet electron density dependence of oscillation amplitude at $T=180$ K and $P=3$, for $N_{depl}=1\times10^{10}$ cm^{-2} (dash-dotted curve) and $N_{depl}=5\times10^{10}$ cm^{-2} (solid curve), where the mobility at vanishing magnetic field is assumed to be 10 000 cm^2/V s and independent of sheet electron density. The solid circles are the experimental data reported by Brummell *et al.* (Ref. 14).

can see in Fig. 9 that Γ_{RIS} increases with increasing N_s. This feature can be explained as the following. Although the screening effect results in a decrease of the broadening as the electron density increases, the Landau-level broadening is dominated by the two factors arising from N_{is} and L_s in Eq. (3.15), leading to an increase in the broadening. The increase in N_s of the samples is achieved by decreasing the spacer layer thickness, which results in an increase in the broadening as shown in Fig. 9. It is straightforward to calculate the amplitude of the MPR oscillations as a function of the sheet electron density when we use the result shown in Fig. 9 and the calculated result is plotted in Fig. 10, where we compared the present result with the experimental date reported by Brummell *et al.*[14] In the calculation, we assumed that the mobility at vanishing magnetic field does not depend on N_s because the phonon limited mobility is almost independent of N_s.[31] We find in Fig. 10 that the calculated amplitude $\Delta\rho/\rho_0$ shows a good agreement with the experimental observation of Brummell *et al.*[14] It is therefore concluded that the electron density dependence of the magnetophonon oscillations is determined by the remote-impurity scattering. It is very interesting to point out that the damping parameter of the magnetophonon resonance in bulk materials is also determined by the impurity scattering as shown by many workers.

We would like to summarize the present work. The magnetophonon resonance in $Al_xGa_{1-x}As/GaAs$ single heterostructures is described by an expression similar to the formula derived by Barker. Our expression is derived by using Fang-Howard trial function and Harmonic analysis. The Landau-level broadening is calculated for the cases of electron scattering by remote-impurity, background-impurity, optical-phonon, acoustic-phonon, and interface-roughness scattering. In the samples we are interested in the broadening is dominated by the remote-impurity scattering. The broadening due to optical-phonon and acoustic-phonon scattering is proportional to square root of the magnetic field, resulting in the magnetic field dependence of the damping parameter γ as inversely proportional to the square root of the magnetic field. The Landau-level broadening due to other scatterings is almost independent of the magnetic field. Therefore the oscillatory structure of the magnetophonon resonance in the samples is well analyzed by assuming a constant Landau-level broadening or a damping parameter γ inversely proportional to the magnetic field and the magnitude of the broadening is determined by the remote impurities.

ACKNOWLEDGMENT

We are grateful to Professor T. Ando, University of Tokyo, for the discussion of the Landau-level broadening.

APPENDIX

We present the approximated expression of Θ which defined by Eq. (2.17) for two cases: (i) degenerate statistics case ($\mu>0$, where μ is the chemical potential) and at temperatures $k_BT>\hbar\omega_0/4$ and (ii) nondegenerate statistics case [$\exp(\beta\mu)\ll1$].

In the first case (i), Θ is given by the following expression:

$$\Theta=\begin{cases}\dfrac{1}{4\tau\hbar\omega_0}(\tau+\mu)^2, & 0<\mu<\hbar\omega_0-\tau \\ \dfrac{\mu+\tau-\hbar\omega_0/2}{2\tau}, & \hbar\omega_0-\tau<\mu<\tau \\ 1-\dfrac{(\tau+\hbar\omega_0-\mu)^2}{4\tau\hbar\omega_0}, & \tau<\mu<\hbar\omega_0+\tau \\ 1, & \mu>\hbar\omega_0+\tau\end{cases} \tag{A1}$$

where $\tau=2k_BT$. We see in Eq. (A1) that Θ is independent of the magnetic field.

In the second case (ii), we obtain the following relation:

$$\Theta=\exp[\beta(\mu-\tfrac{1}{2}\hbar\omega_0)]\frac{\omega_c\sinh(\frac{1}{2}\beta\hbar\omega_0)}{\omega_0\sinh(\frac{1}{2}\beta\hbar\omega_c)} . \tag{A2}$$

[1]T. Ando, A. B. Fowler, and F. Stern, Rev. Mod. Phys. **54**, 437 (1982).

[2]R. Dingle, H. L. Stormer, A. C. Gossard, and W. Wiegmann, Appl. Phys. Lett. **33**, 665 (1978).

[3]T. Mimura, S. Hiyamizu, T. Fujii, and K. Nanbu, Jpn. J. Appl. Phys. **19**, L225 (1980).

[4]J. H. English, A. C. Gossard, H. L. Stormer, and K. W. Baldwin, Appl. Phys. Lett. **50**, 1826 (1987).

[5]R. A. Stradling and R. A. Wood, J. Phys. C **1**, 1711 (1968).

[6]P. G. Harper, J. W. Hodby, and R. A. Stradling, Rep. Prog. Phys. **36**, 1 (1973).

[7]R. L. Peterson, Semicond. Semimet. **10**, 221 (1975).

[8]R. J. Nicholas, Prog. Quantum Electronics **10**, 1 (1985).

[9]R. J. Nicholas, M. A. Brummell, and J. C. Portal, in *Two-Dimensional Systems, Heterostructures, and Superlattices,* edited by G. Bauer, F. Kuchar, and H. Heinrich (Springer-Verlag, Berlin, 1984), p. 69.

[10]D. C. Tsui, Th. Englert, A. Y. Cho, and A. C. Gossard, Phys. Rev. Lett. **44**, 341 (1980).

[11]Th. Englert, D. C. Tsui, J. C. Portal, J. Beerens, and A. C. Gossard, Solid State Commun. **44**, 1301 (1982).

[12]G. Kido, N. Miura, H. Ohno, and H. Sakaki, J. Phys. Soc. Jpn. **51**, 2168 (1982).

[13]M. A. Brummell, R. J. Nicholas, M. A. Hopkins, J. J. Harris, and C. T. Foxon, Phys. Rev. Lett. **58**, 77 (1987).

[14]M. A. Brummell, D. R. Leadley, R. J. Nicholas, J. J. Harris, and C. T. Foxon, Surf. Sci. **196**, 451 (1988).

[15]G. Grégoris, J. Beerens, S. Ben Amor, L. Dmowski, J. C. Portal, F. Alexandre, D. L. Sivco, and A. Y. Cho, Phys. Rev. B **37**, 1262 (1988).

[16]D. R. Leadley, M. A. Brummell, R. J. Nicholas, J. J. Harris, and C. T. Foxon, Solid-State Electron. **31**, 781 (1988).

[17]R. Lassnig and W. Zawadzki, J. Phys. C **16**, 5435 (1983).

[18]F. F. Fang and W. E. Howard, Phys. Rev. Lett. **16**, 797 (1966); F. Stern and W. E. Howard, Phys. Rev. **163**, 816 (1967).

[19]N. Mori and C. Hamaguchi, Technol. Rept. Osaka Univ. **37**, 127 (1987). Reprints are available on request.

[20]P. Warmenbol, F. M. Peeters, and J. T. Devreese, Solid-State Electron. **31**, 771 (1988).

[21]J. R. Barker, J. Phys. C **5**, 1657 (1972).

[22]N. Mori, N. Nakamura, K. Taniguchi, and C. Hamaguchi, J. Phys. Soc. Jpn. **57**, 205 (1988).

[23]R. Kubo, S. J. Miyake, and N. Hashitsume, in *Solid State Physics,* edited by F. Seitz and D. Turnbull (Academic, New York, 1965), Vol. 17, p. 279.

[24]T. Ando and Y. Uemura, J. Phys. Soc. Jpn. **36**, 959 (1974).

[25]P. J. Price, J. Vac. Sci. Technol. **19**, 599 (1981).

[26]S. Das Sarma, Solid State Commun. **36**, 357 (1980).

[27]R. Lassnig and E. Gornik, Solid State Commun. **47**, 959 (1983).

[28]T. Ando, and Y. Murayama, J. Phys. Soc. Jpn. **54**, 1519 (1985).

[29]T. Ando, J. Phys. Soc. Jpn. **51**, 3900 (1982).

[30]C. T. Foxon, J. J. Harris, R. G. Wheeler, and D. E. Lacklison, J. Vac. Sci. Technol. B **4**, 511 (1986).

[31]K. Hirakawa and H. Sakaki, Phys. Rev. B **33**, 8291 (1986).